Identification of Microtubule Binding Sites in the Ncd Tail Domain†

A. Karabay and R. A. Walker*

Department of Biology, Virginia Polytechnic Institute and State University, Blacksburg, Virginia 24061-0406

Received August 3, 1998; Revised Manuscript Received November 16, 1998

ABSTRACT: Nonclaret disjunctional (Ncd) is a minus end-directed, C-terminal motor protein that is required for spindle assembly and maintenance during meiosis and early mitosis in *Drosophila* oocytes and early embryos. Ncd has an ATP-independent MT binding site in the N-terminal tail domain, and an ATP-dependent MT binding site in the C-terminal motor domain. The ability of Ncd to cross-link MTs through the action of these binding sites may be important for Ncd function in vivo. To identify the region(s) responsible for ATP-independent MT interactions of Ncd, 12 cDNAs coding various regions of Ncd tail domain were expressed in *E. coli* as C-terminal fusions to thioredoxin (Trx). Ncd tail fusion proteins (TrxNT) were purified by ion exchange (S-Sepharose) and/or Talon metal affinity chromatography. Purified TrxNT and NT proteins were analyzed in microtubule (MT) cosedimentation and bundling assays to identify which tail proteins were able to bind and bundle MTs. Based on the results of these experiments, all TrxNT and NT proteins that showed MT binding activity also bundled MTs, and there are two ATP-independent MT interaction sites in the tail region: one within amino acids 83−100 that exhibits conformation-independent, high-affinity MT binding activity; and another within amino acids 115−187 that exhibits conformation-dependent, lower affinity MT binding activity. It is possible that both of these MT interacting sites combine in the native protein to form a single MT binding site that allows the Ncd tail to bind cargo MTs in vivo.

The kinesin-like microtubule (MT)[1] motor Nonclaret disjunctional (Ncd) is involved in spindle assembly and maintenance during meiosis in *Drosophila* oocytes and early mitosis in *Drosophila* embryos (*1*−*6*). Ncd translocates toward the minus ends of MTs (*7*, *8*) and is a member of the C-terminal motor group of kinesin superfamily motors (*1*, *2*). Like other kinesin superfamily motors, Ncd is composed of three distinct domains: a conserved motor domain (residues 356−700) that contains the ATP-dependent MT binding site responsible for the force-generating activity of the motor that drives movement; a central stalk region (residues 200−356) of heptad repeats thought to be involved in subunit dimerization; and a tail domain (residues 1−200) thought to be involved in cargo binding and/or regulation of motor activity (*1*, *2*, *8*, *9*).

To date, most research on Ncd and MT motors in general has focused on the motor domain and the mechanisms by which motor proteins move along MTs. In comparison, relatively little is known about the tail domains of these proteins. In the case of Ncd, the sequence of the N-terminal tail domain is unique among kinesin superfamily motors, although like many others, it is positively charged and proline-rich (*1*, *2*, *9*). Based on experiments in which full-length Ncd was found to bundle MTs in vitro (*8*), and in which bacterial-expressed Ncd tail proteins both bound and bundled MTs in vitro (*9*), it has been suggested that the tail of Ncd contains an ATP-independent MT binding site (*8*, *9*). The ability of the tail region to bind MTs and of Ncd to bundle MTs may be important for Ncd function in vivo, and several in vivo observations are consistent with this hypothesis (*3*, *5*, *6*, *8*).

To further define and characterize the region(s) responsible for ATP-independent MT binding of Ncd, we have generated 12 cDNAs encoding various portions of the Ncd tail (NT) domain and expressed the corresponding proteins in *E. coli*. Since previous work with bacterial-expressed Ncd tail proteins found limited solubility (*9*), the tail proteins were produced as fusions with thioredoxin (Trx) in an effort to increase protein solubility. The purified, bacterial-expressed Ncd tail proteins were then analyzed for the ability to bind and bundle MTs both with and without attached Trx (TrxNT and NT proteins, respectively). Based on the results of these experiments, Ncd amino acid sequences 83−100 and 115−187 contain domains that exhibit ATP-independent MT binding activity with high and lower affinity, respectively. The MT interaction site present in the 83−100 sequence is able to interact with tubulin even when the Ncd tail protein is denatured, while the site present in 115−187 appears to be much more sensitive to protein conformation. It is possible that both sequences contribute to MT binding activity in the full-length Ncd motor.

† This work was supported by NIH Grant GM52340 (R.A.W.), a grant-in-aid of research from Sigma-Xi (A.K.), and a Graduate Research Development Project (GRDP) grant (A.K.) from the Graduate Student Assembly at Virginia Polytechnic Institute and State University.

* Corresponding author: Department of Biology, Virginia Polytechnic Institute and State University, Blacksburg, VA 24061-0406. Phone: (540) 231-3803. Fax: (540) 231-9307. E-mail: rawalker@vt.edu.

[1] Abbreviations: MT(s), microtubule(s); Ncd, Nonclaret disjunctional; Trx, thioredoxin; NT, Ncd tail protein; TrxNT, thioredoxin−Ncd tail fusion protein; MAP(s), microtubule-associated protein(s); BSA, bovine serum albumin; IPTG, isopropyl β-D-thiogalactopyranoside.

10.1021/bi981850i CCC: $18.00
Published on Web 01/21/1999

MATERIALS AND METHODS

Construction of NT Plasmids. DNA fragments encoding different regions of the Ncd tail domain were amplified by PCR from the pET-N2 plasmid (*9*). NT1−NT4 were generated by pairing a T7 promoter primer (5′-TAA TAC GAC TCA CTA TAG GG-3′) with specific reverse primers that contained a *Hin*dIII site: P2 (5′-AAG CTT GTT GAG GTC CCT TGA GAG GG-3′); P3 (5′-AAG CTT AAT GCT GGG CAA TGA AGG AGC-3′); P4 (5′-AAG CTT TGT TGC TGT TAT TGA CGA AGG-3′); and P5 (5′-AAG CTT AGC AGC AGC CGC GGC TCC TGA-3′), respectively. NT5−NT9 were produced by pairing specific forward primers that contained an *Eco*RI site: P6 (5′-TCA AGG GAA TTC AAC AAT CTG CCC CAG GTG-3′); P7 (5′-GCC TCC CCA GAA TTC ATG AAG TTG GGC CAC-3′); P8 (5′-AGC GCT GAA TTC ATC AAC GAA CTG CGT GGT-3′); P9 (5′-GCT GCT GAA TTC TTG CCC AGC ATT CCC AGC-3′), and P10 (5′-GCG CCT GAA TTC ATA ACA GCA ACA GCT GTC-3′); respectively, with the P5 reverse primer. Finally, NT10−NT12 were generated by pairing the P6, P7, and P8 forward primers with the P4 reverse primer. Amplified DNA fragments were digested with *Eco*RI and *Hin*dIII and cloned into pET-32 [(pET-32c for NT1−NT4; pET-32a for NT5−NT12 (Novagen)]. NT proteins were expressed as fusions with Trx and contained two 6X His tags, one between Trx and the NT protein and one at the C-terminus of the fusion protein. For all constructs, sequence analysis of both strands confirmed that the inserts were in-frame and of the correct sequence.

Expression and Purification of the NT Proteins. pET-NT plasmid constructs were transformed into BL21(DE3) pLysS host cells for protein expression. Overnight cultures of BL21-(DE3) pLysS cells containing pET-NT constructs were diluted 1:100 into LB media supplemented with ampicillin (100 μg/mL) and chloramphenicol (34 μg/mL), grown at 37 °C until $A_{550} = 0.5-0.7$, and then expression was induced with the addition of 0.25 mM IPTG. After 4 h at 22 °C, cells were pelleted, washed with AB buffer (20 mM Pipes, pH 6.9, 1 mM $MgCl_2$, 1 mM EGTA), and kept frozen at −70 °C. TrxNT proteins were purified by either ion exchange chromatography [S-Sepharose (Pharmacia)]) or metal affinity chromatography [Talon (Clontech)], or a combination of both. For purification on S-Sepharose resin, frozen cells were thawed and resuspended in lysis buffer (20 mM Pipes, pH 6.9, 1 mM $MgCl_2$, 1 mM EGTA, 100 mM NaCl, 1 mM DTT, 1 mM PMSF) including 10 mM $MgCl_2$ and 40 μg/mL DNase I (Boehringer Mannheim). After 30 min on ice, cell lysates were clarified by centrifugation at 20000*g* for 15 min at 4 °C, and the supernatants were further centrifuged at 100000*g* for 15 min at 4 °C. The resulting high-speed supernatants were loaded onto 1 mL S-Sepharose columns preequilibrated with lysis buffer. After washing the column with lysis buffer, bound proteins were eluted with lysis buffer containing 250 mM NaCl (final concentration). Trx, TrxNT1, TrxNT9, and TrxNT12 did not bind to S-Sepharose. Whenever metal affinity chromatography was used, alone or in combination with S-Sepharose chromatography, EGTA was omitted from all buffers, and 0.5 mM β-mercaptoethanol was substituted for DTT; hence, the Talon lysis buffer was composed of 20 mM Pipes, pH 6.9, 1 mM $MgCl_2$, 100 mM NaCl, 1 mM PMSF, and 0.5 mM β-mercaptoethanol. For purification by metal affinity chromatography, high-speed supernatants were prepared using Talon lysis buffer as above and loaded on 1 mL Talon columns. After washing the column with Talon lysis buffer containing 10 mM imidazole, proteins were eluted with Talon lysis buffer supplemented with 150 mM imidazole. In some cases, eluates from S-Sepharose were subjected to further purification with metal affinity resin. After proteins were bound to the Talon resin and the column was washed with Talon lysis buffer containing 250 mM NaCl and/or Talon lysis buffer containing 250 mM NaCl (final concentration) plus 10 mM imidazole, bound proteins were eluted from the Talon resin with Talon lysis buffer containing 250 mM NaCl (final concentration) and 150 mM imidazole. Eluates were dialyzed against AB buffer plus 1 mM DTT. After dialysis, the proteins were stored on ice or quick-frozen in liquid nitrogen and stored at −70 °C. Proteins were concentrated with Centriprep-30 concentrators (Amicon) as needed.

As appropriate, TrxNT fusion proteins were incubated with 1 unit of thrombin per milligram of fusion protein (2 h at 22 °C in AB buffer supplemented with 2.5 mM $CaCl_2$) to cleave the Trx fusion partner (≈13.8 kDa) from TrxNT proteins to generate nonfusion NT proteins. Thrombin was inactivated by addition of EDTA to 5 mM and PMSF to 1 mM, and cleaved proteins were either used immediately or frozen at −70 °C.

MT Binding and Bundling Assays. MT cosedimentation assays were performed in AB buffer containing 40 μM taxol (Calbiochem) and 100 μg/mL bovine serum albumin (BSA). In a reaction volume of 100 μL, TrxNT or NT proteins (typically 5−50 μM final) were mixed with taxol-stabilized MTs (5 μM tubulin final). Control reactions contained no MTs. After incubation for 20 min at 22 °C, reactions were centrifuged at 100000*g* for 30 min at 25 °C through 25% sucrose in AB buffer plus 10 μM taxol. The supernatants were transferred into tubes containing equal amounts of 2× SDS sample buffer, and the pellets were resuspended in 100 μL of 1× SDS sample buffer. Supernatant and pellet fractions were then analyzed by SDS−PAGE or Tricine−PAGE (*10*). For quantitative analysis, the amount of supernatant and pellet samples loaded onto the gels was optimized to ensure a linear relationship between the amount of protein loaded and the intensity of the Coomassie blue stained protein bands. The amount of TrxNT and NT proteins in the supernatant and the pellet fractions was quantified by measuring the protein band intensities relative to standards with AlphaImager 2000 Documentation and Analysis System controlled by AlphaEase version 3.3 software (Alpha Innotech Corp.).

Prior to performing MT binding competition experiments, we determined whether the 20 min incubation time used in the cosedimentation experiments described above was sufficient to allow the binding reaction to reach equilibrium. The TrxNT6 protein (20 μM final) was mixed with taxol-stabilized MTs (5 μM tubulin final) and incubated at 22 °C for up to 120 min. Samples were taken at various times (10, 20, 30, 45, 60, 90, and 120 min), and each sample was subjected to centrifugation as described above except that no sucrose gradient was used. SDS−PAGE and densitometry of Coomassie blue stained proteins were then used to determine the relative amounts of TrxNT6 in the supernatant and pellet fractions for each sample. At each time point, the relative amounts of TrxNT6 in the supernatant and pellet

fractions were identical (data not shown), indicating that the binding reaction reached equilibrium within 10 min. For the actual competition experiments, TrxNT proteins were mixed (see Figure 7 for final concentrations) either simultaneously or sequentially with taxol-stabilized MTs (5 μM tubulin final). For simultaneous addition, two different TrxNT proteins were added, and the reaction was centrifuged after 20 min at 25 °C. For sequential addition, one TrxNT protein was incubated with taxol-stabilized MTs for 20 min, and then a second TrxNT protein was added (diluting the reaction $\leq$5%) and the reaction centrifuged after an additional 20 min incubation at 22 °C.

A MT cosedimentation assay was also used to determine the binding affinity (K_d) and stoichiometry (B_{max}) of selected TrxNT and NT proteins to MTs. In these experiments, the taxol-stabilized MT concentration was kept constant (5 μM tubulin), and the TrxNT or NT protein concentration was varied to obtain different molar ratios of TrxNT or NT to tubulin (from 1:1 to 10:1). The reactions were incubated for 20 min at 22 °C and then subjected to centrifugation (no sucrose gradient was used) and SDS−PAGE as described above. For each protein, the concentration of tail protein in the supernatant and pellet fractions was determined by densitometry of Coomassie blue stained proteins, and K_d and B_{max} were obtained by fitting the data with a rectangular hyperbolae.

TrxNT and NT proteins were assayed for their ability to bundle MTs by mixing taxol-stabilized MTs (5 μM tubulin) with TrxNT or NT proteins at the indicated molar ratios (see Figure 10). After 20 min, a 10 μL sample was removed and prepared for observation by video-enhanced differential interference contrast (VE-DIC) microscopy (*11*).

Blot Overlay Assay. TrxNT1−TrxNT8 proteins were used in blot overlay assays to examine interactions with tubulin. The TrxNT proteins used in blot overlay assay were purified by metal affinity chromatography as described above except that 20 mM Tris-HCl, pH 8.0, 100 mM NaCl, and 8 M urea was used as a denaturing lysis buffer, and proteins were eluted with the same buffer containing 100 mM imidazole. Eluates were further purified by SDS−PAGE using a Mini Prep Cell 491 (BioRad).

Purified TrxNT proteins were separated by SDS−PAGE, transferred to nitrocellulose membranes, and then processed for blot overlay assay as described previously (*12*, *13*) except that AB buffer containing 0.1% (v/v) Tween 20, 0.1% (w/v) gelatin, and 1 mM DTT was used as overlay buffer. After washing with Tris-buffered saline, the blots were processed for immunodetection as described previously (*14*).

Estimation of Native Molecular Weights. Sedimentation coefficients ($s_{20,w}$) were determined by sucrose density gradient centrifugation on a 2.5−10% linear sucrose gradient in AB buffer containing 1 mM DTT. Gradients were centrifuged at 41 000 rpm for 20 h at 4 °C in a Beckman SW 41 Ti rotor. Bovine pancreas trypsin inhibitor (aprotinin) (1 S), horse heart cytochrome *c* (1.9 S), chicken egg albumin (3.66 S), and bovine serum albumin (4.3 S) were used as standards.

Stokes radii (R_s) were determined by gel filtration chromatography using a 90 cm SR-200 gel filtration resin equilibrated with AB buffer containing 200 mM NaCl and 0.02% Tween-20. The column was calibrated with standard proteins of known Stokes radii [horse heart cytochrome *c* (1.2 nm), bovine erythrocyte carbonic anhydrase (2.15 nm), chicken egg albumin (3.05 nm), bovine serum albumin (3.55 nm)]. TrxNT and NT proteins were assayed at a concentration of approximately 50 μM. To determine if these proteins would form oligomers at higher concentrations, a concentration of approximately 120 μM was used. Native molecular weights were calculated as described by Siegel and Monty (*15*) using the equation: $M = (6\pi\eta NR_s s_{20,w})/(1 - \nu\rho)$.

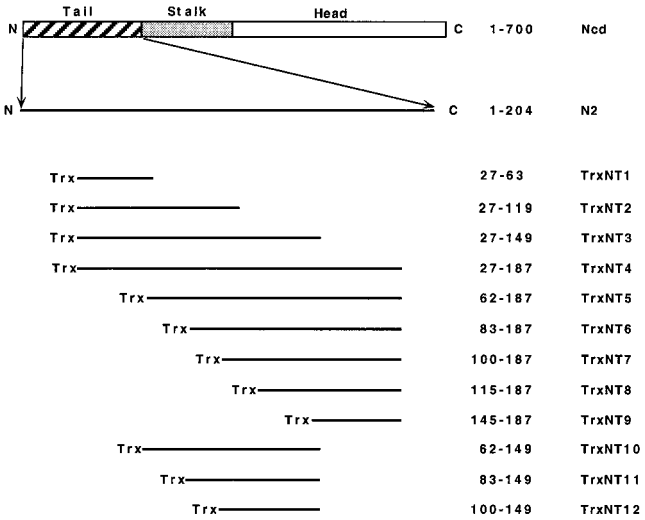

FIGURE 1: Schematic representation of TrxNT proteins. Full-length Ncd consists of 700 amino acids (1). N2 corresponds to the tail region and encodes amino acids 1−204 of Ncd (9). The region encompassed by NT proteins in this study corresponds to amino acids 27−187. TrxNT1−TrxNT4 start from amino acid 27 and include different lengths of deletions at the C-terminus. TrxNT5−TrxNT9 include different lengths of N-terminal deletions in the region starting from amino acid 27. TrxNT10−TrxNT12 contain combined N- and C-terminal deletions. The expected molecular weights are 23 116 (TrxNT1), 29 132 (TrxNT2), 32 122 (TrxNT3), 34 459 (TrxNT4), 31 977 (TrxNT5), 29 805 (TrxNT6), 27 838 (TrxNT7), 26 258 (TrxNT8), 23 243 (TrxNT9), 28 641 (TrxNT10), 26 469 (TrxNT11), and 24 501 (TrxNT12). Trx from pET32 is 20 401 kDa.

RESULTS

Expression and Purification of TrxNT Proteins. To identify and characterize the region(s) responsible for ATP-independent MT binding of Ncd, cDNAs coding various portions of the Ncd tail domain were expressed as fusion proteins with Trx (Figure 1). Upon induction with IPTG, all 12 TrxNT constructs produced proteins of the expected molecular weight. TrxNT1−TrxNT4 were only slightly soluble (10−20%) after lysis, and showed increasing aggregation during attempts at purification by ion exchange or metal affinity chromatography. However, these proteins could be purified to near-homogeneity by a denaturing protocol (see Materials and Methods, Blot Overlay Assay). The other TrxNT proteins remained soluble (80−90%) after lysis and were purified with ion exchange chromatography and/or metal affinity chromatography (Figure 2).

Interaction of TrxNT Proteins with MTs. A MT cosedimentation assay was used to evaluate the ability of the expressed TrxNT proteins to bind MTs (Figures 3 and 4). TrxNT proteins, either partially purified as high-speed supernatants (Figure 3: TrxNT1−TrxNT4) or further purified by column chromatography (Figure 4: TrxNT5−TrxNT12), were combined with MTs and subjected to centrifugation to

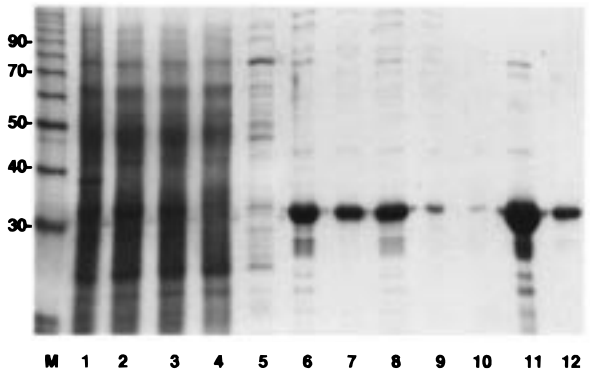

FIGURE 2: Example purification of TrxNT proteins. Bacterial cell lysate (lane 1) induced to express TrxNT6 was centrifuged to produce low-speed (lane 2) and high-speed (lane 3) supernatants as described under Materials and Methods. The high-speed supernatant was then passed over an S-Sepharose column (lane 4 shows proteins that did not bind the resin), and the column was then washed with lysis buffer (lane 5). Bound proteins were eluted (lanes 6 and 7, peak elution fractions), then combined (lane 8), and passed over Talon metal affinity resin (lane 9, flow through). After washing the column (lane 10), bound proteins were eluted with Talon elution buffer (lanes 11 and 12, peak elution fractions). Final eluates from Talon resin were concentrated 50-fold relative to the lysate. Samples were run on a 9% SDS−polyacrylamide gel, and stained with Coomassie Blue. M: Molecular mass marker (indicated in kDa).

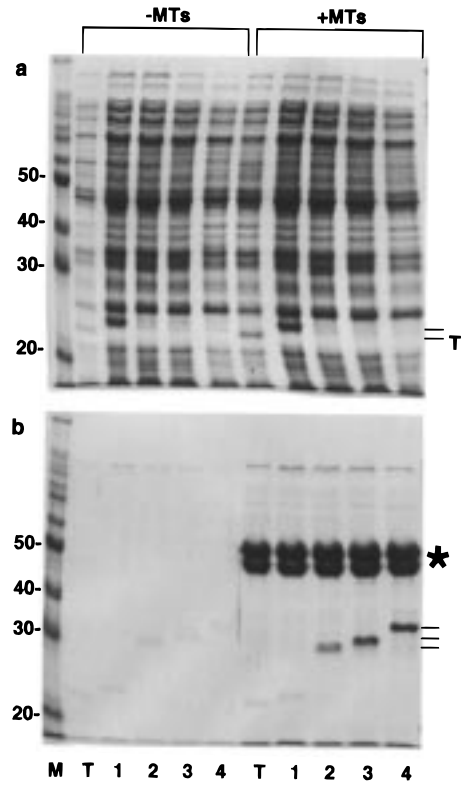

FIGURE 3: MT binding of Trx and TrxNT1−TrxNT4 proteins. High-speed supernatant samples of Trx and TrxNT1−TrxNT4 proteins were divided into two reactions, and taxol and taxol-stabilized MTs were added to one (+MTs), while AB was added to the other (-MTs). After 20 min, the reactions were centrifuged as described under Materials and Methods, and supernatant (panel a) and pellet (panel b) fractions were separated by SDS−PAGE and proteins stained with Coomassie Blue. Lanes 1−4 indicate corresponding TrxNT protein. The positions of thioredoxin (T) and TrxNT1 (horizontal lines) are indicated in panel a, and the positions of TrxNT2−TrxNT4 proteins are indicated (horizontal lines) in panel b. TrxNT2−TrxNT4 bands in panel a supernatant fractions were obscured by endogenous *E. coli* proteins. Tubulin is indicated by an asterisk. Molecular weight markers (M) are indicated in kDa.

separate unbound protein in the supernatant from MT-bound protein in the pellet. Although the exact molar ratio of TrxNT to tubulin in the experiments with high-speed supernatant samples was unknown (Figure 3), it was clear that Trx and TrxNT1 were absent from the MT-containing pellet fractions, indicating that these proteins were unable to bind MTs. In contrast, TrxNT2−TrxNT4 were present in the MT-containing pellet fractions and were completely depleted from the high-speed supernatants, indicating the ability to bind MTs. With column-purified proteins (Figure 4), binding experiments were performed at TrxNT:tubulin molar ratios of 2:1 (TrxNT5, TrxNT6, TrxNT9−TrxNT12) or 4:1 (TrxNT7 and TrxNT8). At these molar ratios, TrxNT5 and TrxNT6 were found entirely in the pellet fraction, small amounts of TrxNT7, TrxNT8, and TrxNT10 were present in the supernatant fractions, and TrxNT11 was distributed equally between the supernatant and pellet fractions. TrxNT9 and TrxNT12 did not show binding to MTs under the same conditions. In control reactions performed in the absence of MTs, little TrxNT protein was found in any pellet fraction. Addition of 5 mM ATP had no effect on the MT binding ability of TrxNT1−TrxNT6.

Binding of TrxNT5, TrxNT6, or TrxNT11 to MTs was unaffected by storage of the protein on ice (1.5 months) or at −70 °C (for as long as 4 months), and was consistent across four separate preparations. In contrast, the MT binding activity of TrxNT7, TrxNT8, and TrxNT10 was unstable with prolonged storage at −70 °C (2.5 months) or storage on ice (1.5 months), and there was complete (TrxNT7 and TrxNT8) or substantial (TrxNT10) loss in MT binding activity under these conditions. There was also significant variability (from binding to complete loss of binding) in the MT binding activity of TrxNT7 and TrxNT8 among seven different preparations, and the binding activity of TrxNT10 showed variability (from binding to reduced binding) only with prolonged storage. All results reported in this paper were obtained with proteins that were stored at −70 °C for no longer than 3 weeks.

The interaction of Trx and TrxNT1−TrxNT8 with unassembled tubulin subunits was examined using a blot overlay assay (*12*, *13*). In these experiments, tubulin subunits were used to probe purified TrxNT proteins (see Materials and Methods) that had been separated by SDS−PAGE and transferred to nitrocellulose (Figure 5). Tubulin interacted with TrxNT2 and TrxNT6, but showed no interaction with Trx, TrxNT1, or, in most cases, TrxNT7. Tubulin was also able to bind TrxNT3−TrxNT5, but generally not to TrxNT8; although occasionally preparation-dependent weak interactions were observed with TrxNT7 and TrxNT8 (data not shown).

To investigate the effect of ionic conditions on the MT binding ability of TrxNT proteins, 0−1 M NaCl was added to reactions containing TrxNT and MTs, and binding was evaluated by a MT cosedimentation assay. Comparative MT binding experiments using 0 and 500 mM NaCl with high-speed supernatants of TrxNT2−TrxNT4 proteins showed that bound TrxNT2−TrxNT4 proteins were almost completely released from MTs in the presence of 500 mM NaCl (data not shown). Comparative MT binding experiments using a

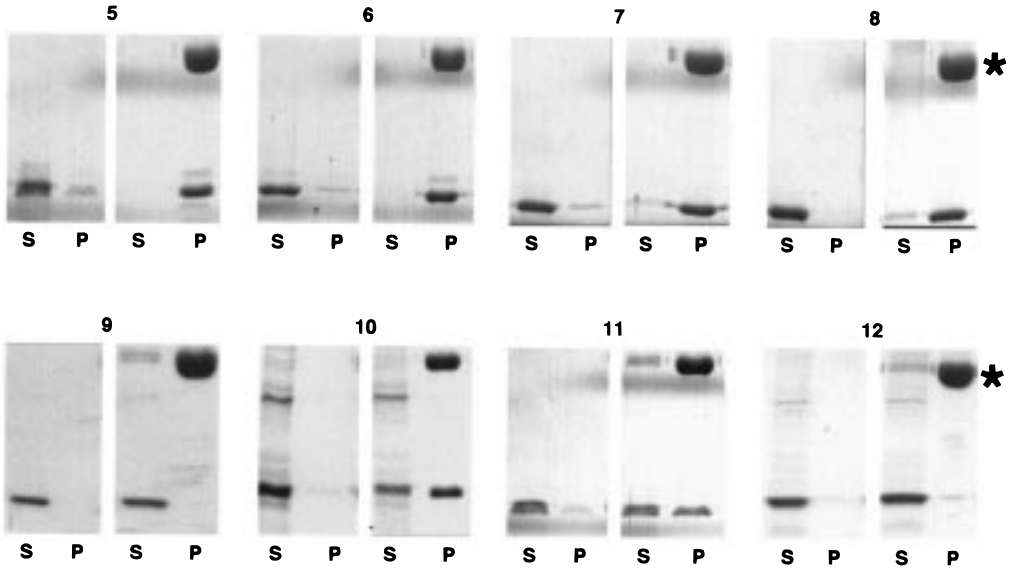

FIGURE 4: MT binding of TrxNT5−TrxNT12 proteins. Column-purified TrxNT proteins were used at 2:1 (TrxNT5, TrxNT6, and TrxNT9−TrxNT12) or 4:1 (TrxNT7 and TrxNT8) molar ratios in a MT cosedimentation assay as described under Materials and Methods. Panel numbers indicate corresponding TrxNT protein. Supernatant (S) and pellet (P) fractions in the absence (left column of each panel) and presence (right column of each panel) of MTs were separated on 8% (panels 5−8, and panel 11), 9% (panels 9 and 12), or 10% (panel 10) SDS−polyacrylamide gels. The location of tubulin in each panel is indicated by an asterisk.

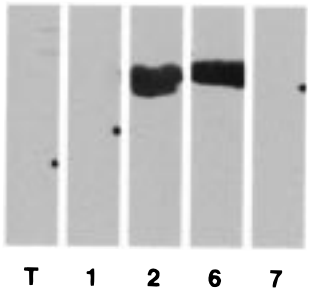

FIGURE 5: Interaction of tubulin with Trx-NT proteins in a blot overlay assay. Column-purified TrxNT proteins were separated by SDS−PAGE, transferred onto nitrocellulose membranes, and processed for overlay with tubulin and subsequent immunodetection as described under Materials and Methods. T: Thioredoxin. Lane numbers indicate the corresponding TrxNT protein, and the dots indicate positions of transferred proteins as detected by Ponceau-S red staining.

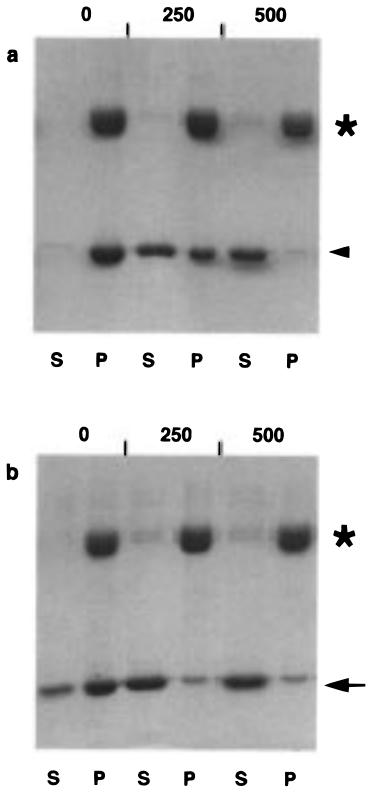

FIGURE 6: Effect of NaCl on TrxNT6 and TrxNT8 binding to MTs. MT cosedimentation assay was carried out as described under Materials and Methods, and the pellets were resuspended with AB buffer containing 40 μM taxol and the indicated NaCl concentration (mM). After 15 min, samples were centrifuged as previously described, and supernatant (S) and pellet (P) fractions were analyzed by SDS−PAGE. Panel a: TrxNT6. Panel b: TrxNT8. The positions of tubulin (asterisk), TrxNT6 (arrowhead), and TrxNT8 (solid arrow) are indicated.

greater range of NaCl concentrations (0, 250, 500, and 750 mM, and 1 M) with TrxNT6 and TrxNT8 resulted in almost complete release of bound TrxNT8 at 250 mM NaCl (Figure 6b), whereas 500 mM NaCl was required to completely release bound TrxNT6 (Figure 6a).

MT binding of selected TrxNT proteins was compared in competition experiments in which two different TrxNT proteins (each at a 4:1 molar ratio to tubulin) were mixed either simultaneously or sequentially with MTs and then subjected to centrifugation (Figure 7). Competition experiments between TrxNT5 and TrxNT6 indicated that if these proteins were added simultaneously, or if either protein was added prior to the other, similar amounts of each protein bound to MTs, suggesting that TrxNT5 and TrxNT6 have similar affinities to MTs. In contrast, TrxNT5 inhibited binding of TrxNT11 to MTs, when TrxNT5 was added either before or simultaneously with TrxNT11. Some binding of TrxNT11 was observed if this protein was added prior to TrxNT5, but the amount of TrxNT11 in the pellet was reduced compared to binding in the absence of competing protein. The competition experiment results with TrxNT5 and TrxNT11 therefore suggested that TrxNT5 has a greater affinity for MTs when compared to TrxNT11. Competition

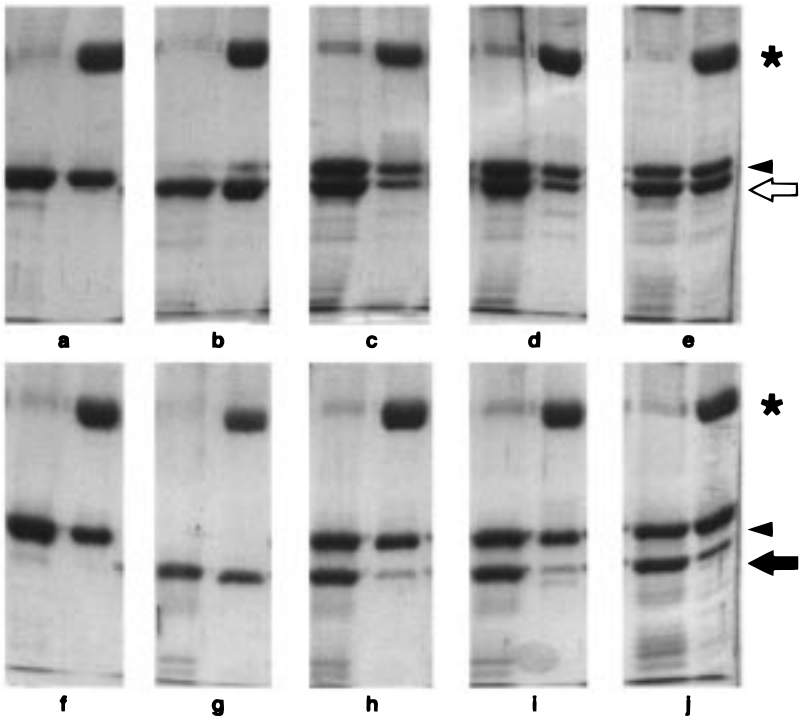

FIGURE 7: Competition of TrxNT proteins for binding to MTs. Column-purified TrxNT5 was added either simultaneously or sequentially with TrxNT6 or TrxNT11, and the binding of each protein was evaluated by MT cosedimentation assay. All proteins were added at a 4:1 TrxNT:tubulin molar ratio. The upper row (panels a−e) shows competition between TrxNT5 and TrxNT6, and the lower row (panels f−j) shows competition between TrxNT5 and TrxNT11. Supernatant (first lane of each panel) and pellet (second lane of each panel) fractions in the presence of MTs are shown. Panels a and f: TrxNT5 alone. Panels b and g: TrxNT6 and TrxNT 11 alone, respectively. Panel c: TrxNT5 and TrxNT6 were added simultaneously. Panel h: TrxNT5 and TrxNT11 were added simultaneously. Panels d and i: TrxNT5 was added prior to TrxNT6 or TrxNT11, respectively. Panels e and j: TrxNT6 or TrxNT11 was added prior to TrxNT5, respectively. The positions of tubulin (asterisk), TrxNT5 (arrowhead), TrxNT6 (open arrow), and TrxNT11 (solid arrow) are indicated.

experiments between TrxNT5 and TrxNT9 demonstrated that TrxNT5 was able to bind MTs without interference from TrxNT9, as expected given the earlier result that TrxNT9 did not bind MTs (data not shown).

To obtain a quantitative measure of the binding of Ncd tail proteins to MTs, various concentrations (5−50 μM final) of representative TrxNT proteins (TrxNT6, TrxNT7, TrxNT8, or TrxNT11) were mixed with MTs (5 μM tubulin) to generate binding reactions at different molar ratios (1:1 to 10:1) of TrxNT to tubulin (Figure 8). After centrifugation to separate supernatants containing unbound TrxNT protein from pellets containing bound TrxNT protein, densitometry of fractions separated by SDS−PAGE was used to determine the concentration of TrxNT protein in both supernatants and pellets (with known amounts of the appropriate TrxNT protein as standards). These data was plotted (Figure 8c) and fit with a rectangular hyperbolae to calculate affinity (K_d) and stoichiometry (B_{max}) values. Using TrxNT6 as an example (Figure 8a,b), almost no TrxNT6 was observed in supernatant fractions at TrxNT6:tubulin ratios of ≤2:1, but TrxNT6 was observed in increasing amounts in the supernatant fractions as the TrxNT6:tubulin ratio was increased from 3:1 to 10:1 (Figure 8a). In comparison, TrxNT6 increased in the pellet fractions as the TrxNT6:tubulin ratio was increased to ≈3:1 and then remained relatively constant at that ratio as the total TrxNT6:tubulin ratio was increased to 10:1 (Figure 8b). A plot of TrxNT6 in the pellet vs TrxNT6 in the supernatant and subsequent fitting of the data with a rectangular hyperbolae generated a calculated K_d of 0.13 ± 0.03 μM and a B_{max} of 15.88 ± 0.48 μM (Figure 8d). Since tubulin was held constant at 5 μM, the calculated B_{max} corresponded to a maximum binding stoichiometry of ≈3:1 TrxNT6:tubulin. Using identical methods, K_d and B_{max} values for TrxNT7, TrxNT8, and TrxNT11 were also calculated (data no shown), and the resulting values are presented in Figure 8d. Based on the calculated K_d values, the relative order of MT affinity for the proteins examined was TrxNT6 > TrxNT11 > TrxNT8 > TrxNT7. This order was consistent with the effects of NaCl observed in Figure 6 and the results of the competition experiments described in Figure 7. The calculated B_{max} values for TrxNT11, TrxNT7, and TrxNT8 indicated that each bound to tubulin at a maximum stoichiometry of ≈4:1 (Figure 8d).

To evaluate the ability of NT proteins without attached Trx to bind MTs, thrombin was added to MT-bound TrxNT proteins to cleave and release the Trx partner, and the effect of cleavage on MT binding was determined. Thrombin treatment of bound TrxNT6 protein had no effect on the ability of NT6 to remain bound to MTs (Figure 9a). When MT-bound TrxNT5, TrxNT10, and TrxNT11 were treated with thrombin, the corresponding released NT proteins also retained MT binding activity. In contrast, thrombin digestion of MT-bound TrxNT8 resulted in loss of NT8 binding to MTs (Figure 9b). Digestion of MT-bound TrxNT7 to generate NT7 gave similar results to those observed for TrxNT8 and NT8. As expected from previous experiments with Trx (Figure 3), the cleaved Trx protein did not bind MTs as indicated by its presence in the supernatant fractions and absence from pellet fractions. TrxNT6 and TrxNT8 were also incubated with thrombin to cleave the Trx partner prior

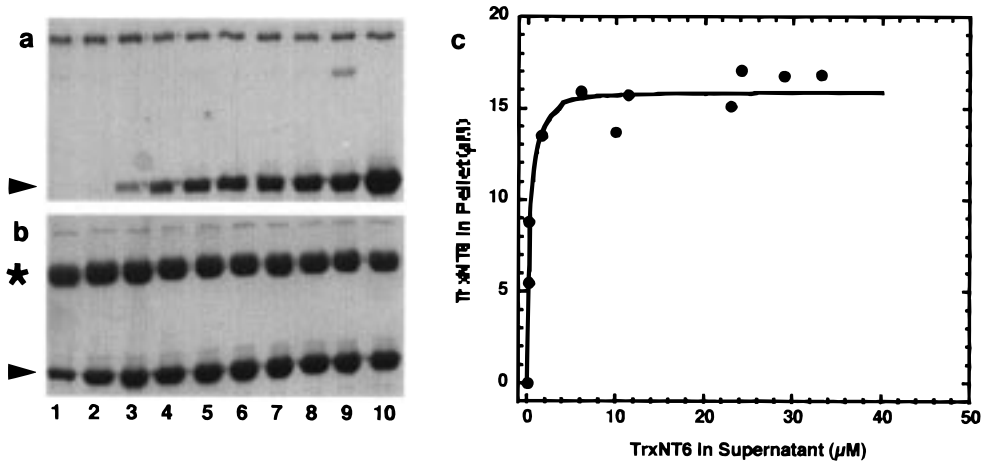

d

	TrxNT6	TrxNT7	TrxNT8	TrxNT11	NT6
K_d (μM)	0.13 ± 0.03	3.2 ± 1.90	2.67 ± 1.21	0.20 ± 0.13	0.09 ± 0.03
B_{max} (μM)	15.88 ± 0.48	20.74 ± 3.48	20.46 ± 2.04	20.55 ± 1.43	19.88 ± 1.17

FIGURE 8: MT binding affinity and stoichiometry of TrxNT6 protein. TrxNT6 (5−50 μM final) was mixed with taxol-stabilized MTs (5 μM final) and centrifuged after a 30 min incubation at 22 °C (see Materials and Methods). Supernatant (a) and pellet (b) fractions were then separated on 10% SDS−polyacrylamide gels, and the amount of TrxNT6 in each fraction was determined. The TrxNT6:tubulin ratio is indicated below panel b for both supernatant and pellet fractions. Tubulin (asterisk) and TrxNT6 (arrowhead) bands are indicated. The bands adjacent to the a and b labels are BSA. The data were plotted as shown in (c) and fit with a rectangular hyperbole to determine K_d and B_{max} values (d). TrxNT7, TrxNT8, TrxNT11, and NT6 (see Figure 9) were examined using the same approach (data not shown), and the calculated K_d and B_{max} values for those proteins are also presented in (d).

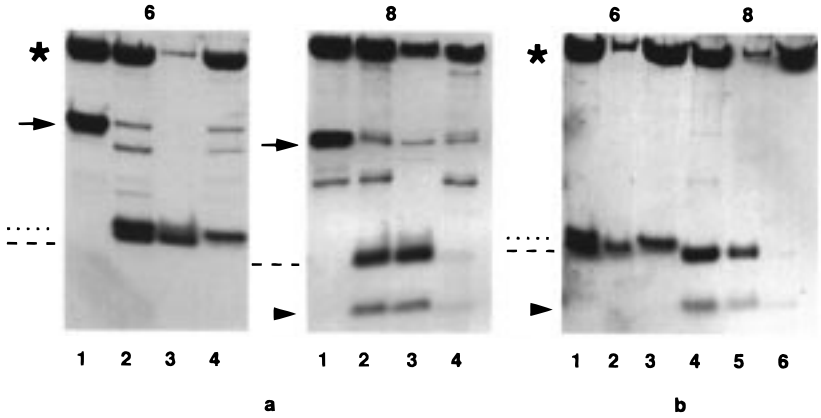

FIGURE 9: MT binding of thrombin-cleaved NT6 and NT8 proteins. To evaluate the binding of NT proteins to MTs, TrxNT6 and TrxNT8 were treated with thrombin either while bound to MTs (a) or prior to incubation with MTs (b). The numbers above the sections of each panel denote the corresponding TrxNT or NT protein (6 or 8) shown. For each protein in panel a, lane 1 shows the pre-thrombin mixture of the TrxNT protein bound to MTs; lane 2 shows the results of thrombin cleavage of each MT-bound TrxNT protein; lane 3 shows the supernatant fraction of each cleaved TrxNT protein after centrifugation; and lane 4 shows the pellet fraction of each cleaved TrxNT protein after centrifugation. In Panel b, lanes 1 and 4 show the initial samples of cleaved NT6 and NT8; lanes 2 and 5 show the supernatant fractions of cleaved NT6 and NT8 after incubation with MTs and subsequent centrifugation; and lanes 3 and 6 show the pellet fractions of cleaved NT6 and NT8 after incubation with MTs and subsequent centrifugation. Samples were separated by Tricine−PAGE and stained with Coomassie Blue. The position of tubulin is indicated by an asterisk. The TrxNT proteins (TrxNT6 or TrxNT8) are indicated by solid arrows, and NT6 (dotted line), NT8 (arrowhead), and thioredoxin (dashed line) are also indicated.

to incubation with MTs in a cosedimentation assay (Figure 9c). After enzymatic treatment, NT6 retained the ability to bind MTs, whereas NT8 lost MT binding activity. Again, Trx showed no MT binding activity and was released to the supernatant fraction. When the binding of NT6, NT7, and NT8 to MTs was quantified as described in Figure 8, K_d and B_{max} values were obtained only for NT6 because NT7 or NT8 did not bind MTs even in the 10:1 reaction. However, the K_d calculated for NT6 (Figure 8d) was similar to that of TrxNT6, and the calculated B_{max} was slightly greater than that of TrxNT6 but the same as the B_{max} determined for TrxNT11, TrxNT7, and TrxNT8 (yielding a NT6:tubulin maximum stoichiometry of ≈4:1).

Since full-length Ncd and the N-terminal 204 residues of Ncd (N2) were previously found to bundle MTs in vitro (*8*, *9*), video-enhanced DIC microscopy was used to examine the ability of the TrxNT proteins to bundle MTs (Figure 10). Reactions were prepared as described under Materials and Methods. High-speed supernatants containing TrxNT1 did not bundle MTs (Figure 10b), while high-speed supernatants

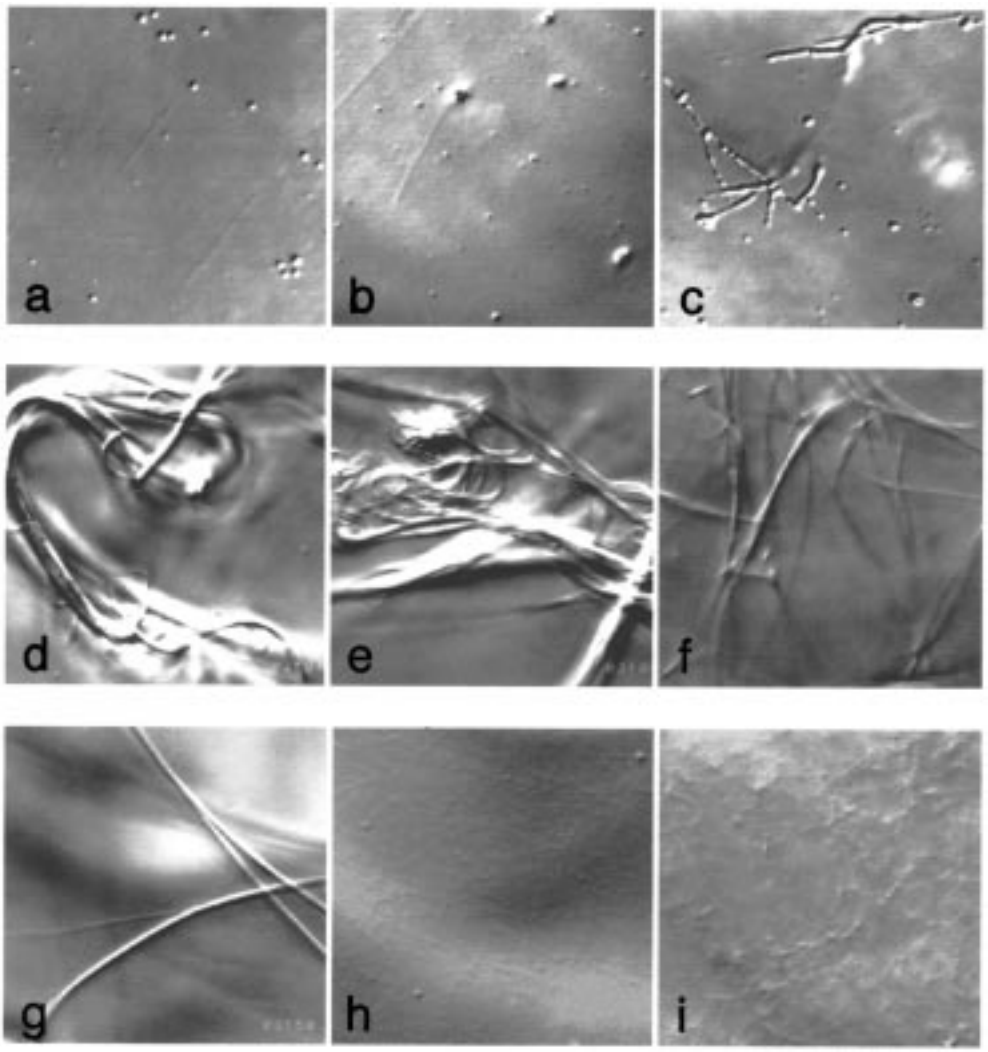

FIGURE 10: MT bundling by selected TrxNT and NT proteins. Panel a: MTs. Panel b: TrxNT1. Panel c: TrxNT4. Panel d: TrxNT6 protein. Panel e: cleavage of MT-bound TrxNT6. Panel f: NT6. Panel g: TrxNT7. Panel h: Cleavage of MT-bound TrxNT7. Panel i: NT7 protein at 2:1 molar ratio. High-speed supernatant samples of TrxNT1 and TrxNT4 were used for MT bundling assay, and samples shown in the upper row were diluted 10-fold before observation. The middle row shows MT bundling ability of TrxNT6 and NT6 used at a 2:1 molar ratio to tubulin. The lower row shows the MT bundling ability of TrxNT7 (panel g) and NT7 (panels h and i) used at 1:1 and 2:1 molar ratios to tubulin, respectively. Each panel is 25 μm wide.

containing TrxNT2, TrxNT3 (data not shown), and TrxNT4 (Figure 10c) produced bundles. Column-purified TrxNT6 (Figure 10d), TrxNT7 (Figure 10g), TrxNT5, TrxNT8, TrxNT10, and TrxNT11 (data not shown) were also able to bundle MTs. At a molar ratio of 1:1 (TrxNT:tubulin), all of the TrxNT proteins that exhibited MT binding activity in the cosedimentation assay (Figure 4), except TrxNT5 and TrxNT10, showed MT bundling activity. TrxNT5 and TrxNT10 started to show MT bundling activity at a 2:1 (TrxNT:tubulin) molar ratio, and at this molar ratio the extent of bundling with TrxNT5 was higher than TrxNT10 based on the presence of single MTs in TrxNT10-containing samples. At very high TrxNT:tubulin molar ratios ($\geq$4:1), it was possible to detect bundling by eye as a fiberlike precipitate in the sample tube. Two main types of bundles were observed: TrxNT7 and TrxNT8 generated linear, cable-like bundles, while the other MT binding TrxNT proteins produced more compact, matted bundles. Based on the number of single MTs observed, TrxNT10 and TrxNT11 were less effective at bundling MTs compared to TrxNT5 and TrxNT6.

To evaluate the ability of NT proteins to bundle MTs, thrombin-treated TrxNT and NT proteins were used in MT bundling assay. Cleavage of MT-bound TrxNT6 (Figure 10e) did not change its bundling activity, whereas cleavage decreased the MT bundling activity of MT-bound TrxNT5 and TrxNT10. Addition of thrombin-released NT6 (Figure 10f) to MTs showed the same extent of bundling as the TrxNT6 fusion protein, although the appearance of the bundles changed from matted structures to long cable-like structures. Based on the number of single MTs, thrombin-released NT5 showed greater bundling activity than released NT10, but not as high as NT6 (data not shown). Cleavage of MT-bound TrxNT7 (Figure 10h) and TrxNT8 resulted in complete loss of bundling activity, and addition of thrombin-released NT7 (Figure 10i) or NT8 to MTs did not produce MT bundling.

To determine whether TrxNT- and NT-induced MT bundling was due to the formation of dimers or oligomers, the sedimentation coefficients and Stokes radii of the MT binding TrxNT and NT proteins were determined and used to estimate native molecular weights (Table 1). When

Table 1: Physical Properties of Ncd Tail Proteins[a]

	Trx-NT				NT			
	polypeptide MW	R_s	$s_{20,w}$	calcd MW	polypeptide MW	R_s	$s_{20,w}$	calcd MW
NT5	31977	35.2	1.9	27597	18209	*<12	1.7	**
NT6	29805	33.8	1.9	26499	16037	*<12	1.5	**
NT7	27838	32.7	1.9	25637	14069	*<12	1.3	**
NT8	26258	32.2	1.9	25245	12489	*<12	1.3	**
NT10	28641	30.1	1.9	23599	14872	*<12	1.3	**
NT11	26469	28.9	ND	ND	12701	*<12	ND	**

[a] Polypeptide MW was determined from the protein sequence. R_s, Stokes radius (Å); $s_{20,w}$, sedimentation coefficient (S). Calculated MW was determined as described under Materials and Methods. (*) Stokes radii of NT proteins were smaller than that of the lowest standard used (horse heart cytochrome, 12 Å); therefore, the precise calculated MW (**) of NT proteins could not be determined. Trx-NT6 and NT6 proteins were each run twice, and other proteins were run once. ND: not determined.

Table 2: Summary of MT Binding and Bundling Assays[a]

(a)

	Trx-NT			Trx-NT	
	binding	bundling		binding	bundling
Trx	−	−	NT7	+	+
NT1	−	−	NT8	+	+
NT2	+	+	NT9	−	−
NT3	+	+	NT10	+	+
NT4	+	+	NT11	+	+
NT5	+	+	NT12	−	−
NT6	+	+			

(b)

	thrombin-cleaved Mt-bound Trx-NT		thrombin-cleaved NT	
	binding	bundling	binding	bundling
NT5	+	+	ND	+
NT6	+	+	+	+
NT7	−	−	ND	−
NT8	−	−	−	−
NT10	+	+	ND	+
NT11	+	ND	ND	ND

[a] Section a indicates MT binding and bundling activities of all Trx-NT proteins. Section b, right column indicates the effect of thrombin cleavage on MT binding and bundling activities of MT-bound Trx-NT proteins. Section b, left column indicates MT binding and bundling activities of cleaved NT proteins. ND: not determined.

compared to molecular weights predicted from amino acids sequences, the calculated molecular weights indicated that TrxNT and NT proteins exist as monomers. Running TrxNT or NT proteins in the presence of DTT, or at concentrations in excess of those used in MT cosedimentation assays (see Materials and Methods), had no effect on the estimated molecular weights.

DISCUSSION

To identify the region(s) in the Ncd tail domain that are involved in ATP-independent binding to MTs, 12 TrxNT proteins corresponding to different regions of the tail domain were expressed in *E. coli*. MT cosedimentation and bundling assays were used to determine the ability of purified TrxNT and thrombin-released NT proteins to interact with MTs. The results (summarized in Table 2) indicate that two sites of MT interaction exist in the Ncd tail domain: one in the sequence from amino acid 83 to 100 and the other in the sequence from 115 to 187.

Evidence in support of amino acids 83−100 containing a MT interaction site is based on the findings that TrxNT2−TrxNT6, TrxNT10, and TrxNT11, as well as the thrombin-released NT5, NT6, NT10, and NT11 proteins, bind and bundle MTs. A lower limit of 83 is indicated since this represents the N-terminal amino acid of NT6 and NT11, while an upper limit of 100 is based on the fact that NT12 does not show MT binding. Consistent with this assignment, blot overlay experiments indicated that TrxNT2−TrxNT6, which contain the 83−100 sequence, interact with tubulin, while those that lack this sequence either have no interaction (TrxNT1) or interact only weakly (TrxNT7 and TrxNT8) with tubulin. The finding that TrxNT2−TrxNT6 proteins purified in the presence of urea and separated by SDS−PAGE were still able to interact with tubulin suggests that the interaction with MTs is not dependent on correct folding of the polypeptide chain to create the binding site. This conclusion is supported by the consistent MT binding activity of TrxNT2−TrxNT6, TrxNT10, and TrxNT11 across multiple protein preparations and varied storage conditions. However, the finding that not all proteins that contain this site bind and/or bundle MTs equally (Figures 7 and 8; Table 2) suggests that, in some of these proteins, the site may either be masked by incorrect folding or binding may be enhanced by a second MT interaction site.

A second site involved in MT binding is present within the Ncd region spanning amino acids 115−187. This conclusion is based on the findings that TrxNT7 and TrxNT8 show MT binding and bundling activity. However, the situation is more complicated than that described previously for the 83−100 sequence. As discussed above, TrxNT7 and TrxNT8 do not interact significantly with tubulin in the blot overlay assay. In addition, TrxNT7 and TrxNT8 showed significant variability in MT binding activity across different protein preparations and after various storage conditions. Further, cleavage of TrxNT7 and TrxNT8 to generate NT7 and NT8 resulted in complete loss of MT binding and bundling activity. Taken together, these results suggest the presence of a conformation-dependent MT interaction site within the Ncd sequence from 115 to 187. The ability of this site to bind MTs is clearly dependent on conditions that affect protein conformation (urea, SDS) and is unstable over time. It is likely that the Trx fusion partner, although unable to bind MTs itself, may aid in stabilizing the NT7 and NT8 conformations and thereby the MT binding activity of these proteins. Thus, cleavage of Trx may trigger a conformational change in NT7 and NT8 that leads to loss of the interaction site and therefore loss of MT binding activity. The presence of aggregated and denatured protein in Figure 10i, in which NT7 had been released by thrombin and then stored at −70 °C prior to the experiment, supports this conclusion. Interestingly, denaturation may be enhanced by freezing and storage

since cleaved NT7, when viewed immediately after digestion, does not appear denatured and aggregated (Figure 10h).

The mechanism by which TrxNT7 and TrxNT8 bind MTs is also complicated by the fact that neither TrxNT9 nor TrxNT12, which together contain the same sequence as TrxNT7 (100−187), binds MTs. One possible explanation for these results is that the conformation-dependent MT interaction site is located in either NT9 or NT12 but is not correctly folded. Alternatively, a bipartite site may be involved in which amino acids in the sequence spanned by NT9 may need to be brought together with amino acids in NT12 by correct folding. Competition experiments (Figure 7) in which TrxNT5 and TrxNT6 showed equivalent affinity for MTs, but TrxNT5 showed greater affinity than TrxNT11, are consistent with either of these possibilities. TrxNT5 and TrxNT6 contain the 83−100 and 115−187 sequences, while TrxNT11 contains the 83−100 sequence but ends at amino acid 149. Thus, it is possible that TrxNT11 is missing either part or all of the conformation-dependent site and that this is the reason for its lower affinity (Figures 7 and 8).

The K_d and B_{max} values obtained for representative Ncd tail proteins (Figure 8) also support the concept of two MT interaction sites. Proteins that contain the 83−100 sequence, and hence the conformation-independent MT interaction site (TrxNT6, NT6, TrxNT11), have a higher affinity for MTs than proteins that contain only the conformation-dependent MT interaction site present in the 115−187 sequence (TrxNT7, TrxNT8). In addition, proteins that contain both sequences (TrxNT6, NT6) have a higher affinity than TrxNT11, which has only the 83−100 sequence. The fact that TrxNT7 and TrxNT8 exhibited reasonably tight binding to MTs, while NT7 and NT8 did not show any MT binding (even at 10:1 molar excess over tubulin), also supports the conclusion that the 115−187 sequence MT interaction site is conformation-dependent. The K_d values calculated for TrxNT6, NT6, and TrxNT11 are similar to or lower than the K_d values reported for the AMP-PNP- or apyrase-induced tight binding of kinesin and Ncd motor domains to MTs (*14*, *16*, *17*,) and the K_d values reported for the binding to MTs of full-length tau and tau fragments that contain the MT binding site (*18*, *19*), and therefore support the concept of a tight, specific interaction. A more surprising result was the B_{max} values and the corresponding NT:tubulin maximum binding stoichiometries of ≈3:1 to ≈4:1. Based on these numbers, it appears that there are four potential binding sites per tubulin dimer (presumably two each per α- and β-tubulin) and that TrxNT6, perhaps due to steric hindrance, cannot fill all possible binding sites. The fact that all proteins for which B_{max} was calculated bind at a ≈4:1 stoichiometry suggests that all are binding to the same sites on tubulin (albeit with different affinities). Further, there was no evidence of cooperative binding, and the data were best fit with a rectangular hyperbolae, suggesting that all four sites on the dimer are identical in terms of affinity (Figure 8c). Given the ionic nature of binding (see following paragraph) and the large number of acidic residues in the C-terminal domains of α- and β-tubulin that are exposed on the outer surface of a MT, it is likely that each of the binding sites on tubulin represents a cluster of acidic residues. Two such clusters are present in both tubulin monomers; one precedes the H12 helix, and the other is present at the extreme C-terminus (*20*). These stoichiometries are higher than reported for other MT binding proteins: motor domains typically saturate at 1 per tubulin dimer (see ref *14*), while tau saturates at 0.5 per tubulin dimer (*19*). This raises the issue of how four separate protein molecules may pack along the dimer. Given the relatively large number of proline residues in the Ncd tail, it is possible that the MT interaction sites protrude from the bulk of the tail domain and that this may allow four proteins to bind to one tubulin dimer without significantly interfering with each other. In addition, if the acidic clusters present in the C-terminal domains of α- and β-tubulin are involved in binding the Ncd tail, the distance between the two clusters in each monomer could be nearly the length (4 nm) of the monomer (*20*), while the distance between clusters on adjacent monomers may vary depending on the flexibility of these regions, and these two factors could allow access to all four sites simultaneously. One final point in considering these stoichiometry values is that Ncd exists as a dimer and this structure may force constraints on the distance between tail domains, making it unlikely that full-length Ncd could fill all possible binding sites on the dimer. Future binding experiments with a stalk−tail dimer of Ncd should help address this issue.

Given the high percentage (17%) of basic amino acids in the 200 amino acids of the Ncd tail domain and the large number of acidic amino acids exposed on the outer surface of MTs (*21*, *22*), it is reasonable to expect that the Ncd tail interaction with MTs is ionic in nature. The effect of NaCl on the MT binding of TrxNT proteins is consistent with this hypothesis (Figure 6). Further, the finding that a higher concentration of NaCl is required to inhibit the MT binding of TrxNT6 as compared to TrxNT8 is consistent with two MT interaction sites (with TrxNT6 having both and TrxNT8 having one). EDC cross-linking between TrxNT7 or TrxNT8 and MTs also supports an ionic interaction (A. Karabay and R. A. Walker, unpublished observations).

In addition to a large number of basic amino acids, the Ncd tail is also rich in proline (22 of 200 or 11%). The abundance of basic amino acids and prolines is a property shared by many MT-associated proteins (MAPs), such as MAP2 and tau, that bind and regulate MT assembly (see refs *23* and *24* for review). MAP2 and tau share 3−4 imperfect amino acid repeats that are involved in binding to MTs. Each repeat is composed of 31 amino acids and contains several basic residues as well as a distinctive Pro-Gly/Lys-Gly-Gly motif (*25*, *26*). A recent study also demonstrated the involvement of the proline-rich region of tau (and by inference, MAP2) in MT binding and provided clear evidence for the importance of specific basic residues (^{215}K, ^{216}K, and ^{221}R) and adjacent proline residues in MT interactions (*24*). Although no repeats are obvious in the Ncd tail, there are clusters of basic residues flanked by proline residues. Analysis of the Ncd 83−100 sequence (^{83}MKLGH-RAKLRRSRSACDI^{100}) indicates that this region contains six basic residues (or 33% of the region) and has two adjacent proline residues (^{80}PEP^{82}). Additional basic clusters are also present in the Ncd sequence from 115 to 187 in the following regions: ^{104}RGNKR^{108}, ^{121}KVSR^{124}, ^{135}RLVR^{139}, and ^{150}VKRPPVTRPAPRAAGGAAAKKPAGTG^{175}. The nearest proline residues to the 104−108 and 121−124 clusters are ^{116}PSIP^{119}, while ^{139}PAAP^{142} are closest to the 135−139 cluster. The largest cluster, residues 150−175, contains six basic residues as well as two adjacent (^{139}PAAP^{142}) and four

internal proline residues (^{153}PPVTRPAP^{160}). The internal proline residues are part of a sequence in Ncd (^{151}KRPPVTR^{157}) that is similar to the MT binding sequence in the proline-rich region of tau (^{215}KKVAVVR^{221}) (*19*). The relationship between the basic and proline clusters in Ncd and tau/MAP2 is unclear and awaits further characterization of the specific amino acids involved in MT binding. However, in preliminary experiments using video microscopy and cosedimentation assays, we have found that TrxNT6 and NT6 promote MT assembly (A. Karabay and R. A. Walker, unpublished observations). Of related interest, Kar3, another C-terminal kinesin superfamily motor, may also interact with MTs via the tail domain (*22*). The tail region of Kar3 resembles that of Ncd in terms of the percentage of prolines (8.2%) and basic (16.4%) amino acids, and similar regions of basic residue clusters with adjacent proline residues are present within amino acids 5−80 of the Kar3 tail (*27*).

As implied above, and consistent with TrxNT1's failure to bind MTs, amino acids 27−63 do not appear to contain a MT binding site. However, this region does appear to affect the solubility of expressed NT proteins. Fusion to Trx did not substantially improve the solubility of the constructs that contained amino acids 27−63 (TrxNT1−TrxNT4). TrxNT2−TrxNT4 were consistently insoluble in different preparations, while TrxNT1 showed variable solubility in different preparations. In comparison, TrxNT proteins which did not contain this region showed greater solubility. Protein sequence analysis showed that this region is rich in hydrophobic and polar-uncharged amino acids and has only three charged amino acids (R^{28}, R^{59}, and D^{60}).

All TrxNT proteins that bound MTs also bundled MTs, and all NT proteins that retained MT binding ability after thrombin cleavage were also able to bundle MTs (Table 2). The differences in the structure (cable-like with TrxNT7 and TrxNT8, matted with all other TrxNT and NT proteins that showed MT binding activity) and extent (more free MTs with TrxNT7, TrxNT8, TrxNT10, TrxNT11, NT10, and NT11 than TrxNT5, TrxNT6, NT5, and NT6) of MT bundling may be an indication of differences in the stability and/or accessibility of MT interaction sites. Alternatively, these differences may be a function of having one versus two of the MT interaction sites.

How do TrxNT and NT proteins induce MT bundling? One possible mechanism could be dimerization of the proteins to form cross-bridges between MTs. However, based on the results of gel filtration and sedimentation experiments (Table 1), TrxNT and NT proteins appear to exist as monomers. Although this does not exclude the possibility that TrxNT and NT proteins may form dimers or oligomers in the presence of MTs, it is also possible that the proteins form bundles by shielding charges. As discussed above, it is likely that the positively charged MT binding sites in the Ncd tail interact with the negatively charged C-terminus of α- and/or *β*-tubulin. It has been proposed that MT bundling could result from the neutralization of the acidic carboxyl-terminal region of tubulin, which can be achieved by binding of MAPs including tau (*28*, *29*). Consistent with this hypothesis, binding of the monomeric motor domain of Ncd to MTs can also induce MT bundling (K. Phelps and R. A. Walker, unpublished results). Hence, it is possible that TrxNT and NT proteins form bundles not by physically connecting separate MTs, but rather by masking tubulin domains that otherwise inhibit MT bundling. Although bundles could be formed in vitro by charge neutralization, it is likely that MT bundling as part of spindle organization in vivo would occur through a mechanism in which the motor domains of Ncd interact with one MT and the tail domains interact with a second MT, and thereby cross-link the two filaments.

In conclusion, there appear to be two regions in the Ncd tail that can interact with MTs. Given the importance of protein conformation in one of these regions, it is likely that MT binding is not simply due to nonspecific charge interactions, but rather that structural complexity is important for MT binding. Intramolecular interactions between basic and proline-rich regions may bring these two MT interaction sites together in the folded protein to form a single MT binding site. Thus, determination of the 3D structure of the Ncd tail region should help elucidate the interactions of the tail domain with MTs. In the future, site-directed mutagenesis experiments will also be needed to determine the amino acid residues essential for MT binding. Finally, since Ncd has not yet been purified from native cells, it is conceivable that the MT interaction of the tail region could be regulated by nonmotor subunits or associated proteins.

ACKNOWLEDGMENT

We thank Dr. Sharyn A. Endow for her generous gift of the pET/N2 plasmid that was used in this study.

REFERENCES

1. Endow, S. A., Henikoff, S., & Soler-Niedziela, L. (1990) *Nature 345*, 81−83.
2. McDonald, H. B., & Goldstein, L. S. B. (1990) *Cell 61*, 991−1000.
3. Hatsumi, M., & Endow, S. A. (1992) *J. Cell Sci. 103*, 1013−1020.
4. Endow, S. A. (1993) *Trends Genet. 9*, 52−55.
5. Matthies, H. J. G., McDonald, H. B., Goldstein, L. S. B., & Theurkauf, W. E. (1996) *J. Cell Biol. 134*, 455−464.
6. Endow, S. A., and Komma, D. J. (1997) *J. Cell Biol. 137*, 1321−1336.
7. Walker, R. A., Salmon, E. D., and Endow, S. A. (1990) *Nature 347*, 780−782.
8. McDonald, H. B., Stewart, R. J., and Goldstein S. B. (1990) *Cell 63*, 1159−1165.
9. Chandra, R., Salmon, E. D., Erickson, H. P., Lockhart, A., and Endow, S. A. (1993) *J. Biol. Chem. 268*, 9005−9013.
10. Schagger, H., and Jagow, G. V. (1987) *Anal. Biochem. 166*, 368−379.
11. Walker, R. A., O'Brien, E. T., Pryer, N. K., Soboeiro, M. F., Voter, W. A., Erickson, H. P., and Salmon, E. D. (1988*) J. Cell Biol. 107*, 1437−1448.
12. Boucher, D., Larcher, J.-C., Gros, F., and Denoulet, P. (1994) *Biochemistry 33*, 12471−12477.
13. Larcher, J.-C., Boucher, D., Lazereg, S., Gros, F., and Denoulet, P. (1996) *J. Biol. Chem. 271*, 22117−22124.
14. Walker, R. A. (1995) *Proc. Natl. Acad. Sci. U.S.A. 92*, 5960−5964.
15. Siegel, L. M., and Monty, K. J. (1965) *Biochim. Biophys. Acta 112*, 346−362.
16. Crevel, I. M.-T., Lockhart, A., and Cross, R. A. (1996) *J. Mol. Biol. 257*, 66−76.
17. Moore, J. D., Song, H., and Endow, S. (1996) *EMBO J. 15*(*13*), 3306−3314.
18. Goode, B., and Feinstein, S. C. (1994) *J. Cell Biol. 124* (5), 769−782
19. Gustke, N., Trinczek, B., Biernat, J., Mandelkow, E.-M., and Mandelkow, E. (1994) *Biochemistry 33*(*32*), 9511−9522.

20. Nogales, E., Wolf, S. G., and Downing K. H. (1998) Nature *391*, 199−203.
21. Sackett, D. L., and Wolff, J. (1986) *J. Biol. Chem*. *261*, 9070−9076.
22. Britling, F., and Little, M. (1986) *J. Mol. Biol*. *189*, 367−370.
23. Delacourte, A., and Buee L. (1997) *Int. Rev. Cytol. 171*, 167−210.
24. Goode, B. L., Denis, P. E., Panda, D., Radeke, M. J., Miller, H. P., Wilson, L., and Feinstein, S. C. (1997) *Mol. Biol. Cell 8*, 353−365.
25. Lewis, S. A., Wang, D., and Cowan, N. J. (1988) *Science 242*, 936−939.
26. Ennulat, D. J., Liem, R. K. H., Hashim, G. A., and Shelanski M. L. (1989) *J. Biol. Chem*. *264*, 5327−5330.
27. Meluh, P. B., and Rose, M. D. (1990) *Cell 60*, 1029−1041.
28. Scott, C. W., Klika, A. B., Lo, M. M. S., Norris, T. E., and Caputo, C. B. (1992) *J. Neurosci. Res*. *33*, 19−29.
29. Brandt, R., and Lee, G. (1993) *J. Cell Biol. 268*, 3414−3419.

BI981850I